

# Defect annealing of neutron-irradiated silicon crystals

MENG XIANG-TI, ZUO KAI-FEN

*Institute of Nuclear Energy Technology, Tsinghua University, Beijing 100084, People's Republic of China*

Doppler broadening positron annihilation spectroscopy has been used to investigate the effects of neutron integrated flux and hydrogen on annealing behaviour of defects in silicon crystals. The concentration of neutron radiation defects was estimated, activation energy of some annealing stages was calculated and some specific annealing phenomena were explained.

## 1. Introduction

It is well known that a lot of radiation-induced and secondary defects such as interstitial silicon atoms, vacancies, vacancy-impurity complexes and disordered regions are produced since neutrons collide with silicon atoms and radiation defects combine with impurity atoms in neutron-irradiated silicon. The study of annealing behaviour of radiation defects has been an important subject [1, 2], but there are often big differences between reported results because of different radiation conditions, starting materials and measurement methods. Therefore, a detailed study of defects in neutron-irradiated silicon is still very necessary for a better understanding of fundamental defect nature in semiconductors and technological application.

Hydrogen is one of the most important impurities in silicon. It can react with defects and cause many important solid state phenomena. Hydrogen passivation of defects and impurities is of major practical importance. The study of effects of hydrogen in silicon is also an interesting and notable area [3]. In general, hydrogen is introduced by means of proton-implantation and hydrogen plasma methods.

Since positrons are very similar to hydrogen atoms, positron annihilation technology (PAT) is advantageous for studying the effect of hydrogen on defect annealing of silicon.

The lineshape parameter obtained from Doppler broadening measurements depends on the electron momentum distribution at the defect site, which is characteristic of the trapping defects. In a vacancy-type defect the density of valence electrons is reduced, leading to the narrowing of their momentum distribution which is seen as an increase in the *S*-parameter. The change in the *S*-parameter is proportional to the trapping fraction. Under some circumstances it is possible to track changes in defect type and/or defect concentration by monitoring changes in the Doppler lineshape parameter.

In the present work, hydrogen in silicon is introduced in the process of crystal growth. We present the results of Doppler broadening measurements on neutron-irradiated floating-zone silicon grown in

argon atmosphere and in hydrogen atmosphere, and subsequently annealed from room temperature (RT) to 1200 °C, discuss the annealing behaviour of defects as well as the effects of neutron integrated flux and hydrogen on it.

## 2. Experimental procedure

The  $\phi 12 \times 1$  (mm) samples were cut from an *n*-type floating-zone Si single crystal ingot grown in argon atmosphere-FZ(Ar) Si and in hydrogen atmosphere-FZ(H<sub>2</sub>) Si with the resistivities of 1500 and 180 Ω cm, and with the interstitial oxygen concentrations of  $1.5 \times 10^{17} \text{ cm}^{-3}$  and  $1.8 \times 10^{17} \text{ cm}^{-3}$  respectively, determined by FTIR. The hydrogen concentration in sample H is  $1.1 \times 10^{17} \text{ cm}^{-3}$  [4]. The neutron irradiation was performed at RT in a light-water reactor of Institute of Nuclear Energy Technology, Tsinghua University with total neutron integrated flux of  $6 \times 10^{16}$  (for sample A1),  $3.6 \times 10^{17}$  (for samples A2 and H2) and  $1.2 \times 10^{18}$  neutrons  $\text{cm}^{-2}$  (for sample A3). The 20 min isochronal annealing from RT to 1150 °C was carried out in argon atmosphere. Then the sample surfaces were polished for measurements.

The Doppler broadening of the annihilation line was measured using an intrinsic Ge detector with energy resolution better than 1.18 keV at the 497 keV line. About  $2 \times 10^6$  counts were recorded for each spectrum, repeated at least 10 times. The lineshape of spectra was characterized by the *S*-parameter, which is defined as the ratio of the counts in the central region of the annihilation line to the total number of the counts in the spectrum.

## 3. Results and discussion

### 3.1. Influence of neutron dose on defect annealing

Since the *S*-parameter is a measurement of annihilation probability of positrons and valence electrons and gives the average effect about the formation and recovery of defects, its value is almost unaffected by artificial computer analysis.

The  $S$ -parameters of FZ(Ar) Si and neutron-irradiated FZ(Ar) Si with three neutron integrated fluxes as a function of annealing temperature are shown in Fig. 1. Here, the experimental error for the  $S$ -parameter is within  $\pm 0.0004$ .

The  $S$ -parameter of as-grown FZ(Ar) Si is 0.501.

Since trapping in open-volume defects decreases the width of the Doppler-broadening energy spectrum, the  $S$ -parameter of neutron-irradiated Si is generally greater than that of as-grown silicon.

The  $S$ -parameter of as-irradiated samples A1, A2 and A3 increases to 0.5044, 0.5142 and 0.5177, respectively. The increase in  $S$ -parameter indicates that an increasing fraction of positrons is trapped and that the concentration of vacancy-type defects increases with increasing neutron integrated flux.

According to Ref. [5], the displaced atoms induced by fast neutrons, thermal neutrons,  $\beta$ - and  $\gamma$ -ray irradiations in the reactor are estimated to be  $1.5 \times 10^{17}$ ,  $9 \times 10^{17}$  and  $3 \times 10^{18} \text{ cm}^{-3}$  in samples A1, A2 and A3, respectively.

We can roughly estimate the change of concentration of defects ( $C_d$ ) in Si using measured  $S$ -parameters [6], also

$$C_d = (\lambda_f/\mu)(S - S_f)/(S_d - S) \quad (1)$$

where  $\mu$  is the specific trapping rate for positrons into the defect, taking  $5 \times 10^{14} \text{ s}^{-1}$  due to monovacancy-type defects for unirradiated Si and the average  $\mu$  value  $7.5 \times 10^{14} \text{ s}^{-1}$  from those of neutral divacancies and monovacancy-type defects [7] because they coexist in neutron-irradiated Si;  $\lambda_f$  is the annihilation rate in defect free silicon and is the inverse of the bulk positron lifetime 219 ps,  $S_f$  and  $S_d$  are the contributions from the free and trapped positrons, respectively. We take the  $S$  value 0.4999 of as-grown FZ Si as  $S_f$ , and take a maximum  $S$  value 0.5192 of FZ(H<sub>2</sub>) Si irradiated with a high integrated flux of  $1.2 \times 10^{18} \text{ neutrons cm}^{-2}$  and annealed at 250 °C as  $S_d$  since it should be relatively near the saturation value obtained for high defect concentrations where most of the positrons should be trapped. Here  $S_d/S_f = 1.039$ , which is nearly the same as the previously reported value of 1.038 [8].

The estimated defect concentration is  $3 \times 10^{16}$ ,  $9.5 \times 10^{16}$ ,  $8.86 \times 10^{17}$  and  $3.63 \times 10^{18} \text{ cm}^{-3}$  in as-grown FZ(Ar) Si and as-irradiated samples A1, A2 and A3 respectively, using Equation 1. Possibly the value is slightly large for sample A3 since the  $S_d$  value is taken from that of Si irradiated with a high neutron integrated flux, and the defect concentration is not high enough to be a saturation value. If we assume that the increase of defect concentration is proportional to neutron integrated flux, the  $S$  value of sample A3 should be  $3 \times 10^{18} \text{ cm}^{-3}$ , in comparison with that of sample A2. This value is just equal to the value estimated above according to Ref. [5].

As shown in Fig. 1, during annealing the  $S$ -parameter of FZ(Ar) Si only changes slightly, indicating that a small quantity of vacancy-type defects still exist in as-grown Si, and rearrangement and/or interaction with impurity atoms (e.g. oxygen atoms). As we know, the oxygen-related donors or thermal donors are

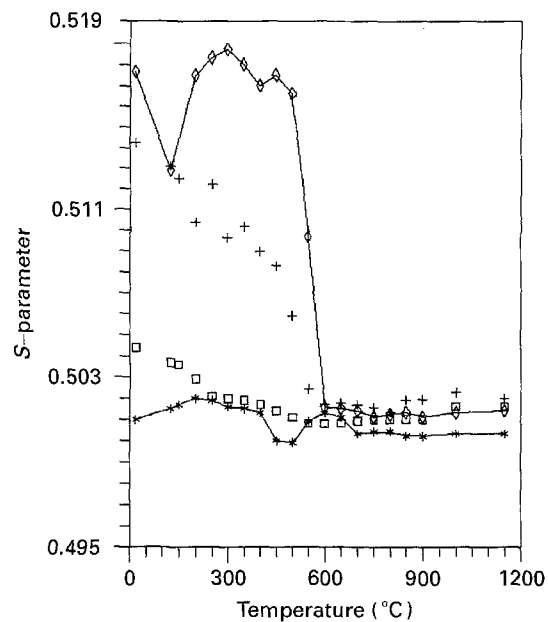


Figure 1 The  $S$ -parameter of FZ Si grown in argon atmosphere and neutron-irradiated FZ Si with three neutron integrated fluxes as a function of annealing temperature.  $\diamond$  Sample A3;  $+$  Sample A2;  $\square$  Sample A1;  $*$  Fz (Ar) Si.

produced in Si oxygen-containing annealed at 400–500 °C. A substitutional oxygen-vacancy model for thermal donors ( $\text{O}_{\text{Si}}^+ \text{V}_n^-$ ) has been proposed [9]. The formation of thermal donors can impede positrons annihilating in the ionized donors and cause the decrease of the  $S$ -parameter since positrons are non-sensitive to positively charged species. Therefore, the  $S$ -parameter has a visible decrease at 450–500 °C. At annealing temperatures higher than 700 °C the  $S$ -parameter remains nearly constant.

The dependence of the annealing behaviour of positron-sensitive defects on neutron integrated flux appears clearly in Fig. 1.

For sample A1 irradiated with  $6 \times 10^{16} \text{ neutrons cm}^{-2}$  two annealing stages can be observed: one from RT–250 °C, and another from 250–550 °C.

For sample A2 irradiated with  $3.6 \times 10^{17} \text{ neutrons cm}^{-2}$  three annealing temperature ranges can be shown: RT–200 °C, 200–300 °C and 350–600 °C; for sample A3 irradiated with  $1.2 \times 10^{18} \text{ neutrons cm}^{-2}$  RT–125 °C, 125–400 °C and 400–600 °C.

The vacancy-phosphorus (V-P) complexes can be produced in  $\beta$ -decay process of  $^{31}\text{Si}$  atoms formed owing to thermal neutron capture of  $^{30}\text{Si}$  atoms; its concentration is about  $1 \times 10^{13}$ ,  $6 \times 10^{13}$  and  $2 \times 10^{14} \text{ cm}^{-3}$  in as-irradiated samples A1, A2 and A3. The V-P complexes anneal out at 120–180 °C [10]. The negatively charged divacancy-oxygen ( $\text{V}_2\text{-O}^-$ ) complexes also begin to anneal from about 120 °C [11]. Some interstitial silicon atoms can annihilate in the annealing temperature range between 100–150 °C [10] due to their recombination with vacancy-type defects. The annealing stage of neutral divacancies ( $\text{V}_2^0$ ) at 100–200 °C in neutron-irradiated silicon has been proposed to be due to approach of interstitial defects to divacancies localized in the cores of neutron radiation disordered regions [12]. Those can be the

reasons of the first annealing stage at RT–250 °C for sample A1, at RT–200 °C for sample A2 and at RT–125 °C for sample A3. The activation energy of annealing for sample A1 from RT–250 °C and sample A2 from RT–200 °C was calculated to be 0.18 eV and 0.26 eV respectively. The migration activation energy of negatively charged  $V^-$  was reported to be 0.18 eV [13] and neutral  $V^0$  0.25 eV [14]. Our results show that migration of monovacancies dominates this annealing stage. Here, we note that sample A1 is *n*-type due to small defect concentration but sample A2 is *p*-type because its Fermi energy level locates nearly in the middle of forbidden band gap.

It should be noticed that the obvious increases in *S*-parameters upon annealing at 200–250 °C for sample A2 and at 125–300 °C for sample A3 were observed. This “reverse annealing” is generally considered to be typical of materials containing disordered regions [15]. The growth of the positron-sensitive defects can be attributed to the formation of  $V_2$ -O complexes [7] and divacancies due to them in disordered regions becoming “visible” for positrons [16] and/or aggregation of monovacancy-type defects released from disordered regions.

From electron paramagnetic resonance (EPR) data [2] divacancies are thought to start migrating at about 177 °C and to disappear at about 350 °C. The  $V_2$ -O complexes also disappear at about 350–400 °C [7, 17]. This explains the decrease in *S* value from 250–300 °C for sample A2 and from 300–400 °C for sample A3.

It is interesting to note that the onset of the reverse annealing stage moves towards lower temperatures with increasing neutron integrated flux. This is related to the formation of secondary divacancies and  $V_2$ -O complexes. No obvious secondary defects form in sample A1 irradiated with low neutron integrated flux because of residual monovacancies, and those released from disordered regions are too small to aggregate and form into divacancies and  $V_2$ -O complexes. The concentration of monovacancies and divacancies in Si increases with increasing neutron integrated flux. The mask of the concentration increase of secondary defects on first annealing stage can explain the above phenomenon.

For sample A1 the *S*-parameter decreases gradually from 250–550 °C mainly owing to annealing out of  $V_2$ -O complexes [17]. For samples A2 and A3, however, irradiated with larger neutron integrated flux the annealing behaviour becomes much more complicated. After secondary divacancies reach the maximum concentration, the *S*-parameter decreases due to annealing out of  $V_2$ -O and  $V_2$  defects, but increases again at 350 and 450 °C for samples A2 and A3, respectively, and a “shoulder” at 450 °C for sample A2 is visible. Those are due to the formation of high-order multivacancy clusters such as quadrivacancies ( $V_4$ ) and pentavacancies ( $V_5$ ) as well as more complicated vacancy-oxygen (e.g.  $V_3$ -O) complexes. The calculated activation energy of annealing above 450 °C is 0.85 and 0.97 eV for samples A2 and A3, respectively. This agrees with that of migration of interstitial silicon atoms, 0.85 eV, reported previously [10]. This also

shows that migration of interstitial atoms and their recombination with vacancies play an important role in the annealing process above 450 °C. For sample A3 the *S*-parameter still is very high at annealing temperatures lower than 500 °C. The *S*-parameter decreases suddenly to 0.5016 at 600 °C which is nearly the same as that for unirradiated Si. This shows that most of radiation defects and secondary defects have been removed.

The *S*-parameters of neutron-irradiated Si annealed above 600 °C change very little and are near the values of, but a little bigger than, those of unirradiated Si.

### 3.2. Effect of hydrogen

Fig. 2 is the *S*-parameter of samples A2 and H2 irradiated with  $3.6 \times 10^{17}$  neutrons  $\text{cm}^{-2}$  versus annealing temperature curve.

The effect of hydrogen on annealing behaviour of defects is very obvious. In the first annealing stage the *S*-parameter of hydrogen-containing Si drops to a minimum value at 150 °C, lower by 50 °C than that of sample A2; the minimum value is much smaller than that of sample A2. The *S*-parameter decreases by 29% for sample A2 but by 44% for sample H2 from RT to the valley. This can be attributed to hydrogen passivation of acceptor centres such as V-P,  $V_2$ -O and  $V_2$  defects. The neutralization of the acceptor centres decreases the specific trapping rates at defects and thus the apparent concentration of positron-sensitive defects and *S*-parameter.

During the reverse annealing the *S*-parameter of hydrogen-containing sample H2 increases to the maximum value at a lower temperature, 200 °C, and this *S* value is much smaller than that of sample A2, indicating that hydrogen minimizes the formation of secondary defects.

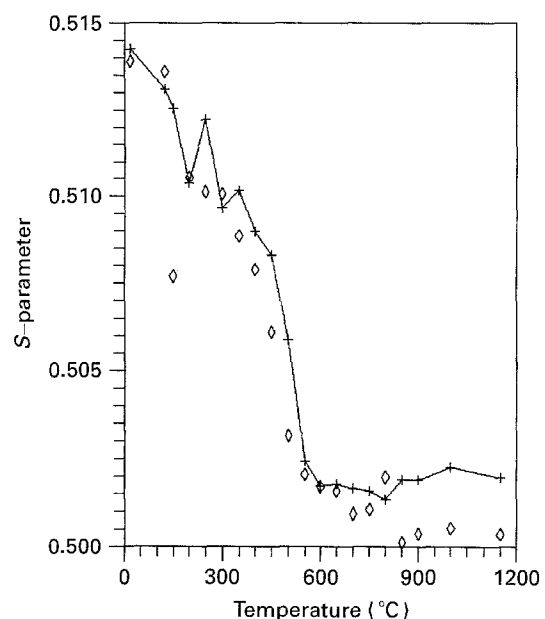


Figure 2 The *S*-parameter of FZ Si grown in argon atmosphere and hydrogen atmosphere and irradiated with  $3.6 \times 10^{17}$  neutrons  $\text{cm}^{-2}$  as a function of annealing temperature. + Sample A2; ◇ Sample H2.

At annealing temperatures higher than 300 °C, the *S*-parameter of sample H2 also decreases gradually with increasing annealing temperature and to nearly the same value as that of unirradiated Si at 600 °C. But the *S*-parameter is smaller by 13, 12, 26, 47 and 15% than that of sample A2 at 350, 400, 450, 500 and 550 °C, respectively. The calculated activation energy of annealing from 300–550 °C from *S*-parameters is 0.486 eV. This value is in good agreement with that for hydrogen diffusion [18]. This result shows that hydrogen facilitates annealing out of vacancy-type defects. Hydrogen atoms possibly take part in the intermediate stage of the recombination of vacancy–interstitial atoms. In addition, the hydrogen–defect shallow donor forms just in this temperature range [19]. The vacancy-type defects participating in the formation of hydrogen shallow donors would be seen for positrons.

#### 4. Conclusion

The Doppler broadening positron annihilation measurements show that the defect concentration of as-grown FZ Si and neutron-irradiated FZ Si with  $6 \times 10^{16}$ ,  $3.6 \times 10^{17}$  and  $1.2 \times 10^{18}$  neutrons  $\text{cm}^{-2}$  is estimated to be  $3 \times 10^{16}$ ,  $9.5 \times 10^{16}$ ,  $8.86 \times 10^{17}$  and  $3 \times 10^{18}$   $\text{cm}^{-3}$  respectively. The activation energy of the first annealing stage from RT–200 °C is 0.18–0.26 eV. The onset of the reverse annealing stage moves towards lower temperatures with increasing neutron integrated flux due to different concentrations of secondary  $V_2$ –O and  $V_2$  defects. The activation energy of annealing above 450 °C is 0.85–0.97 eV, indicating that migration of interstitial atoms and their recombination with vacancies play an important role in this annealing stage.

Hydrogen significantly affects the first annealing stage owing to its passivation on acceptor centres; it minimizes the formation of secondary defects such as  $V_2$  and  $V_2$ –O complexes; the fact that the secondary defects in hydrogen-containing Si are easy to remove and the activation energy of annealing above 300 °C is 0.486 eV suggests that hydrogen motion probably controls the annealing process.

#### Acknowledgements

The author would like to thank Professor T. B. Zhang and Dr W. Puff for help in positron annihilation measurements.

#### References

1. B. B. GOSSICK, *J. Appl. Phys.* **30** (1959) 1214.
2. L. J. CHENG, J. C. CORELLI, J. W. CORBETT and G. D. WATKINS, *Phys. Rev.* **152** (1966) 761.
3. H. J. STEIN, *Phys. Rev. Lett.* **43** (1979) 159.
4. X. T. MENG, G. G. QIN, Y. C. DU and Y. F. ZHANG, *J. Appl. Phys.* **63** (1988) 5606.
5. J. M. MEESE, in "Neutron transmutation doping in semiconductors" Edited by J. M. Meese (Plenum, New York, 1978) p. 1.
6. B. NIELSEN, O. W. HOLLAND, T. C. LEUNG and K. G. LYNN, *J. Appl. Phys.* **74** (1993) 1636.
7. P. MASCHER, S. DANNEFAER and D. KERR, *Phys. Rev. B* **40** (1989) 11764.
8. J. MAKINEN, E. PUNKKA, A. VEHANEN, P. HAUTOJÄRVI, J. KEINONEN, M. HAUTALA and E. RAUHALA, *J. Appl. Phys.* **67** (1990) 990.
9. D. HELMREICH et al., in "Semiconductor silicon", *J. Electrochem. Soc.*, **PV-77-2** (1977) 626.
10. L. S. SMIRNOV, "A survey of semiconductor radiation technology (Mir Publishers, Moscow, 1983) p. 18.
11. M. KWETE, D. SEGERS, M. DORIKENS, L. DORIKENS-VANPRAET and P. CLAUWS, *Phys. Status Solidi A* **122** (1990) 129.
12. I. V. ANTONOVA, A. V. VASIL'EV, V. I. PANOV and S. SHARMEEV, *Sov. Phys. Semicond.* **23** (1989) 671.
13. G. D. WATKINS, J. R. TROXELL and A. P. CHATTERJEE, in "Def. and Rad. Eff. in Semicond." Proceedings of the International Conference, Nice, France, 1978 (Institute of Physics, London, 1979) p. 16.
14. S. N. ERSHOV, V. A. PANTELLEV, S. N. NAGOMYKH and V. V. CHERNYAKHOVSKII, *Sov. Semicond. Phys.* **19** (1977) 187.
15. A. K. PUSTOVOIT, R. F. KOVOPLEVA, A. I. KUPCHISHIN and K. M. MUKASHEV, *Ibid.* **3** (1989) 160.
16. L. J. CHENG, C. K. YEH, S. I. MA and C. S. SU, *Phys. Rev. B* **8** (1973) 2880.
17. S. MAKINEN, H. RAJAINMAKI and S. LINDEROTH, *Ibid.* **42** (1990) 11166.
18. A. VAN WIERINGEN and N. WARMOLTZ, *Physica* **22** (1956) 849.
19. X. T. MENG, G. T. DU and K. M. LIU, *Nucl. Sci. Eng.* **2** (1982) 172.

Received 15 December 1993  
and accepted 3 February 1995